This article has been accepted for publication in a future issue of this journal, but has not been fully edited. Content may change prior to final publication. Citation information: DOI10.1109/TMRB.2022.XXXXXXX, IEEE Transactions on Medical Robotics and Bionics

Development of an Optical Shape Sensing method using Optoelectronic Sensors for Soft Flexible Robotic Manipulators in MIS

Dalia Osman[1], Xinli Du[1], Wanlin Li[2], Yohan Noh[1]

(1) Dept. of Mechanical and Aerospace Eng., Brunel University London, UB8 3PH, United Kingdom (2) Centre for Advanced Robotics @ Queen Mary (ARQ), Queen Mary University London, E1 4NS, United Kingdom. e-mail: dalia.osman@brunel.ac.uk and yohan.noh@brunel.ac.uk (corresponding author)

***Abstract*— this paper presents the novel design of an optical shape sensing method using optoelectronic sensors, for integration into flexible soft robotic manipulators, to measure pose in two orientations. Shape sensing in soft robotic tools that allow stable and accurate position control in Minimally Invasive Surgery is critical, although innovations are yet to be explored in a simple, cost-effective sensing technique. Presented in this work is a continuation of the work of Koh et.al [1], with demonstration of the use of a designed 4-plate tendon-actuated flexible manipulator and optimised design parameters for the sensing principle. Developed calibration platform shows an increase in accuracy for shape sensing using linear and non-linear regression models. Further development is required on miniaturisation to refine accuracy and targeted application.**

Index Terms —Shape Sensing, Optoelectronic Sensor, Soft Robotics, Calibration, MIS

I. Introduction

The employment of soft robotics in the field of Minimally Invasive Surgery (MIS) has been transformative in the practice of medicine, and innovation has led to the development of a multitude of soft flexible robotic manipulators. Shape sensing in robotics is a key part of accurate and stable closed loop position control during actuation, crucial for safe use in MIS procedures through tortuous anatomical paths involving delicate tissue prone to rupture. Common position tracking in MIS has traditionally been done using imaging modalities, such as MRI, CT, Fluoroscopy and Ultrasound. These provide excellent image resolution that help the surgeon guide tools inside the body, although take up large room, requiring expensive computational image reconstruction, and can expose patients to excess amounts of radiation[2]. Newer developments lead to shape tracking being an intrinsic feature of the surgical tool utilised. Structurally variant soft continuum robots such as tendon actuated, concentric tube, pneumatic continuum robots, adopted different shape sensing principles. Mounted cameras and endoscopes have been utilised extensively and can provide the surgeon with live internal images; however, these have blind spots where the anatomy is more complex and block the line of sight. Innovative tracking sensors such as inertial, radiofrequency coils and electromagnetic sensors [3] [4] have shown promising position tracking accuracy, although component size and interference with external medical equipment may limit its capacity for a range of procedures. Optical based shape sensing is common. Schmitz et al. used modulation of light intensity using optical fibre cables along sections of a snake-like manipulator [5], where light reflected at unit sections was collected using phototransistors at the base. The varying voltage signals induced by the phototransistor were used in machine learning models to reconstruct the robot's shape. Al Jaber et al used a similar approach, using a camera to capture images of

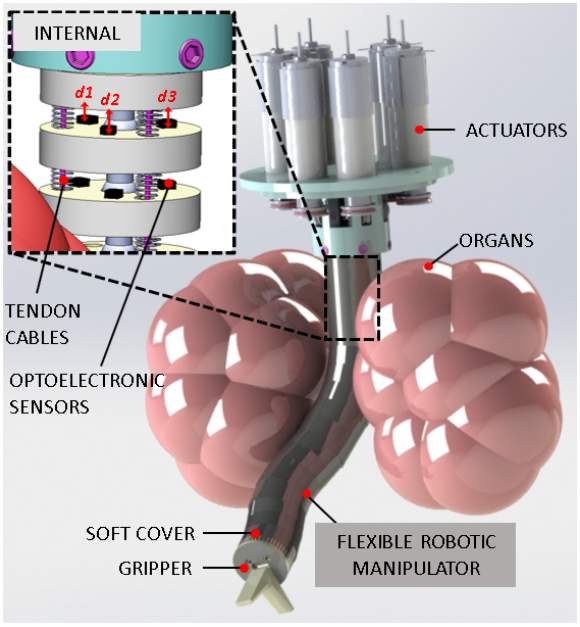

Fig. 1. Concept Image: Optoelectronic sensors deployed in tendon actuated soft robot. Bending will modulate light reflected to sensor and vary the output voltage

fluctuating light [6]. When considering such methods for a full-length robotic manipulator, each segment would accumulate a number of these optical fibres which would increase the overall stiffness and size of the continuum robot. Sareh et al demonstrated an optical sensing method using optical fibre macro bend stretch sensors [7] around the length of a soft robot arm, although large tool tip estimation errors reported were assumed to have arisen from limits to bending angle as well as signal loss from external pressure. A popular optical technique for shape sensing in soft robotics is the use of Fibre Bragg Gratings (FBGs). These are small gratings typically fused inside optical fibres. Variation in strain due to bending in the fibre modulates the wavelength of light passing through the gratings [8]. The technique has been proved a very accurate method of shape tracking particularly in applications such as biopsy needles as well as continuum robots [9]. Shi shows FBGs integrated into an aortic catheter for valve implantation to measure orientation in just a 2D planar case [10]. Three-dimensional shape sensing using FBGs placed into tendon driven continuum robots, such as in [11] and [12], have proved that FBGs have very advantageous characteristics. Features such as miniature dimensions, biocompatibility and the flexibility granted when mounted onto an optical fibre, with increased accuracy when utilising more FBG units, make them one of the most suitable options for narrow continuum robotic structures for applications in MIS. However, the notable difficulty in engraving the gratings and fusing accurately into

This article has been accepted for publication in a future issue of this journal, but has not been fully edited. Content may change prior to final publication. Citation information: DOI10.1109/TMRB.2022.XXXXXXX, IEEE Transactions on Medical Robotics and Bionics

optical fibres during manual manufacture was found in these cases to be a source of error in shape estimation. FBGs are also sensitive to temperature drift, and as well as a shift in the central wavelengths over time, which must be accounted for by calibration[13]. FBG sensing also presents increased error in low stiffness conditions, since the use of more compliant material for larger deflection also increases compliance in torsion[12]. Also, FBG based shape sensing cannot be integrated into extensible continuum robots [14]. Along with manufacturing of FBG sensors, and the cost of peripheral equipment such as an interrogator, total cost of the system can sum upwards of £10k (HMBshop)[5]. In keeping with the optical methods, the work in this paper demonstrates an alternative solution for shape sensing in soft robotic tools for MIS using optoelectronic sensors. These sensors are integrated into discs of a tendon actuated flexible robot and are used to derive a pose measurement system in two orientations, by mapping reflected intensity modulated voltage signals to orientation based on the degree of bending of each consecutive disk. The proposed sensing modality possesses a great number of advantages as follows. The electrical circuit and mounting of the sensing units (£0.32/sensor) can be produced using a printed circuit board, so fabrication is much simpler and cheaper in comparison with conventional shape sensing methods. The method employed would not have signals disturbed by external electromagnetic fields and displays low noise where ambient light can be blocked. Sensors display a large voltage variation without requirement for an amplifier, while the optical properties ensure a high sampling rate. The technique offers a simple, small, biocompatible system that does not intrinsically depend on curvature limiting properties such as strain or temperature and can be adapted to work with different continuum robotic structures. Koh et al [1] showed early stages of this work, presenting a shape sensing method using optoelectronic sensors integrated within 3-plates of a tendon actuated flexible robot (Fig. 1). However, a calibration platform able to adjust two orientations (pitch and roll) was not fully conceived, thus manual calibration led to errors during the calculation of the calibration matrix. In addition, linear regression applied during calibration resulted in inaccuracy, due to inherent nonlinear characteristic profiles of displacement vs output voltage of the optoelectronic sensors. The aim of this paper is to overcome these issues, by proposing a new automated calibration platform for increased accuracy through calibration, with non-linear mapping models explored in comparison with linear regression on an extended 4-plate tendon actuated manipulator.

II. MATERIALS AND METHODS

A. Design Requirements

Surgical robotic tools for MIS have a set of specific requirements, although greatly depend on the intended procedure. In this work, our sensing modality is focused on integration into a section of a multi-backbone continuum robot. In MIS, the diameter of these robots ranges between 10mm to 15mm, for commercially available trocar ports of this size [15]. In terms of workspace, at least two orientations and a bending angle range of more than 90° is typical. Tip accuracy is again task dependent, though tool tip orientation errors of 0.5-2° have been accepted [16]. While the prototype in this work is larger for purposes of studying the sensing principle (W = 32mm, H = 140mm), future prototypes will be minimised and lengthened for such targeted application. Given these requirements, a tendon actuated robotic structure that integrates optoelectronic sensors with advantages described in the introduction, will make a suitable sensing principle for MIS applications. This will be done through optimising sensor configuration, designing a new calibration platform using actuators that can obtain pure orientation data (pitch and roll), and combining this information with sensor data through linear and non-linear regression models to find a calibration matrix that can guarantee a highly accurate orientation estimation.

B. Sensing Principle

The basis of how the sensing principle works for the proposed shape sensing system within a tendon actuated robot is illustrated in Fig 1 and 2. As shown in Fig.2, triplets of optoelectronic sensors are placed equilaterally on each plate at a radius of 10mm, of which are jointed using socket-ball joints. These constrain spatial motion, while three fitted springs between each plate limit the torsion (twist), overall allowing bending in both pitch (β) and roll (γ) orientations. The optoelectronic sensors utilised (QRE113 ON Semiconductor, 3.6 x 2.9 x 1.7 mm) are comprised of a coupled light emitting diode (LED) and Phototransistor. By using the upper plate as a reflective surface for each sensor, the degree of bending of each plate will modulate the intensity of reflected light as distance *d* changes between this upper plate and the sensor (Fig.1), which varies the voltage output of the sensors. Passing sets of voltage values from each plate through a regression algorithm can map them to an orientation in two directions, giving a transformation matrix for consecutive plates that can be used to estimate the final pose at the tip of the manipulator. In this way a simple shape sensing system can be developed for a tendon actuated robotic manipulator.

C. Actuation

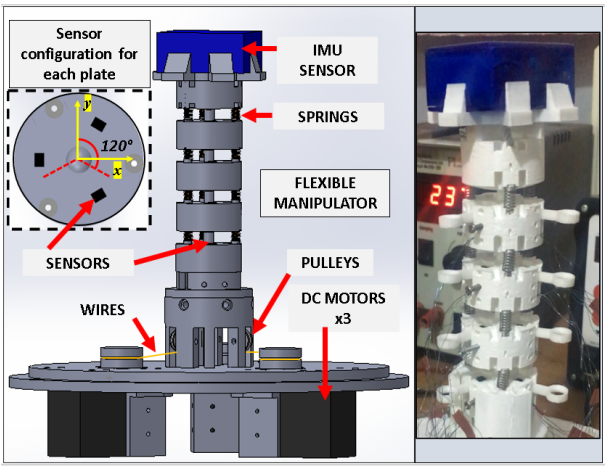

Fig. 2 Four plate tendon driven robotic manipulator with integrated optoelectronic sensors within plates. Tendons are driven using 3 motors

A tendon actuated flexible manipulator was used as the structure to house the sensing system in this study. Motor control software was developed using Python to control the three tendon pulling DC motors (Dynamixel XL430-W250T). Tendon lengths were calculated using a vector-based model

This article has been accepted for publication in a future issue of this journal, but has not been fully edited. Content may change prior to final publication. Citation information: DOI10.1109/TMRB.2022.XXXXXXX, IEEE Transactions on Medical Robotics and Bionics

[17]. Given an input target orientation of the top plate relative to the base, the model was used to calculate the required tendon lengths, and then converted to three target motor positions. As the three motors move simultaneously, each pulls a tendon wire over the pulley for continuous motion. For initial optimization experiments, the structure consisted of just one base plate with an upper plate for surface reflectance (Fig. 4). However further experiments, as described in following sections, consisted of four-unit plates which served as a continuous bending section of a flexible robot (Fig.2). An inertial measurement unit (IMU) (LPMS B, LP-RESEARCH Inc, Tokyo, Japan) was fixed above the top plate to provide orientation information at the tip location. The platform was designed using CAD software (Solidworks) and 3D printed using white PLA (Polylactic Acid) plastic.

D. Optimisation

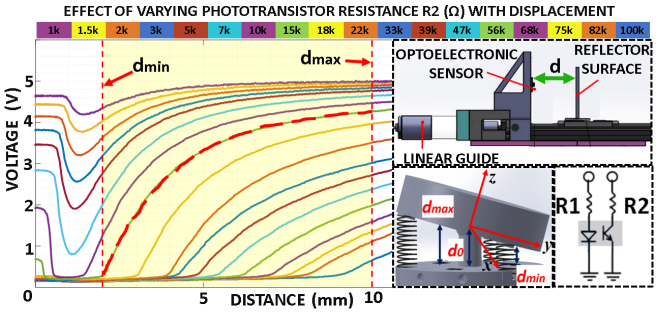

Fig. 3 Left: Sensor output with varying phototransistor resistor values (R2), to find large voltage variation. Right: Optimisation experiment set-up; linear guide for moving set distance while recording sensor output.

To construct the prototype manipulator integrated with optoelectronic sensors, the design and configuration of the sensors and the robot had to be established. As depicted in Fig.3, the distance between sensor and upper plate (d_{min} - d_{max}) during rotation must be within the sensing range and optimized for increased sensor sensitivity for maximised accuracy during calibration. This was done by undertaking an initial sensor study to understand output characteristics when changing distance linearly between the sensor and a reflector. Fig 3 (right) shows the experiment set up consisting of a motorised linear guide, where the sensor is fixed on one end, and a flat surface reflector is mounted onto the moving platform. Software was used to input a selected displacement for the moving platform to travel away from the sensor while the sensor voltage values were recorded. By testing different resistor configurations in the sensor circuit, that is, phototransistor resistor R2 (Fig 3), the voltage variation over this displacement could also be varied. The graph in Fig 3 shows the results of multiple variation curves over 0 – 15mm displacement, where each time the R2 value was changed. Results showed that a curve with large output range was demonstrated by the R2 = 15kΩ configuration, while R1 was selected at 150Ω, which corresponded to a displacement range of 2-10mm (d_{min} - d_{max}). The displayed large voltage range would support sensor sensitivity in subsequent calibration experiments. Therefore, the robotic manipulator discs had to be designed in a way the angular range of each disc would conform to the boundaries of the linear displacement range (2-10mm), when considering displacement between this disk and the lower sensor housing disk; otherwise, the sensor signal would saturate if the upper disk surface were too far, or a very low signal would be registered due to exceeded proximity during rotation. By setting the initial distance between plates to 6.5mm (d_0), ±15° was found to be this angular range within which this displacement boundary would be upheld when the full motion of the plate was completed in both orientations. This is for example seen in Figure 4 in section II.E, showing the full sensor data for all orientations during calibration of one of the plates. In this way, as much of the sensor range was used as possible, and the shape sensing method could be fully explored in terms of its capabilities.

E. Single Unit Calibration

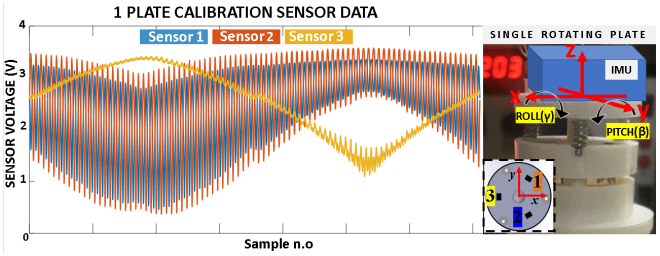

Fig.4 Graph (left) - Full sensor data recorded for calibration motion of one plate (right) with IMU to recorded ground truth value.

Once the design for the manipulator and sensor configuration were optimized, the next step was to test the calibration algorithm. This was first done using just one rotating plate, as in Fig.4, using the tendon-driven platform described in Fig.2. The base plate was fixed while the upper plate, through programmed control by software, rotated over a full angular range between ± 15 ° in both orientations, pitch, and roll simultaneously, in steps of 0.1° while the sensor data was recorded. This provided a comprehensive set of optoelectronic sensor data that covered all combinations of pitch and roll within the range. The IMU mounted on top of the upper plate was used to measure actual angular data for pitch and roll to serve as ground truth data. Fig. 4 shows all the sensor data collected for the three sensors over this motion pattern. For the calibration, this data was first passed through a linear regression model, using the set of sensor values with ground truth data of the IMU sensor. With the improved and automated calibration technique compared to [1], the aim was to compare previous linear regression results to the current results to validate that the calibration method has indeed been cause for an improvement in estimation accuracy. While linearity as a sensor property is desirable in terms of stability, it was evident that the sensor variation curves of output voltage vs displacement in Fig.3 were not linear. For this reason, a nonlinear regression model was also used. Shown in the linear model in Eq (1), pitch and roll are calculated using a set of three coefficients per orientation, of matrix (k), multiplied by the set of sensor values (v_1, v_2, v_3) . Eq (2) shows the nonlinear model, where a series of 16 coefficients per orientation are multiplied by the model to estimate β^i and γ^i, for each plate (i). Results are shown in Fig 6 comparing the two regression models.

$$\begin{bmatrix} k_{11}^i & k_{12}^i & k_{13}^i \\ k_{21}^i & k_{22}^i & k_{23}^i \end{bmatrix} \begin{bmatrix} v_1^i \\ v_2^i \\ v_3^i \end{bmatrix} = \begin{bmatrix} \beta^i \\ \gamma^i \end{bmatrix} \quad (1)$$

$$i = 1,2,3,4$$

This article has been accepted for publication in a future issue of this journal, but has not been fully edited. Content may change prior to final publication. Citation information: DOI10.1109/TMRB.2022.XXXXXXX, IEEE Transactions on Medical Robotics and Bionics

$$\gamma^i, \beta^i = K_1^i + K_2^i + K_3^i \quad (2)$$

where,

$$K_1^i(v_1, v_2, v_3) = k_1^i v_1^i + k_2^i v_2^i + k_3^i v_3^i$$

$$K_2^i(v_1, v_2, v_3) = k_4^i {v_1^i}^2 + k_5^i {v_2^i}^2 + k_6^i {v_3^i}^2 + k_7^i v_1^i v_2^i + k_8^i v_1^i v_3^i + k_9^i v_3^i v_2^i$$

$$K_3^i(v_1, v_2, v_3) = k_{10}^i v_1^i {v_2^i}^2 + k_{11}^i v_2^i {v_1^i}^2 + k_{12}^i v_1^i {v_3^i}^2 + k_{13}^i v_3^i {v_1^i}^2 + k_{14}^i v_3^i {v_2^i}^2 + k_{15}^i v_2^i {v_3^i}^2 + k_{16}^i {v_1^i}^2 {v_2^i}^2 {v_3^i}^2$$

$$i = 1,2,3,4$$

F. Four Unit Calibration

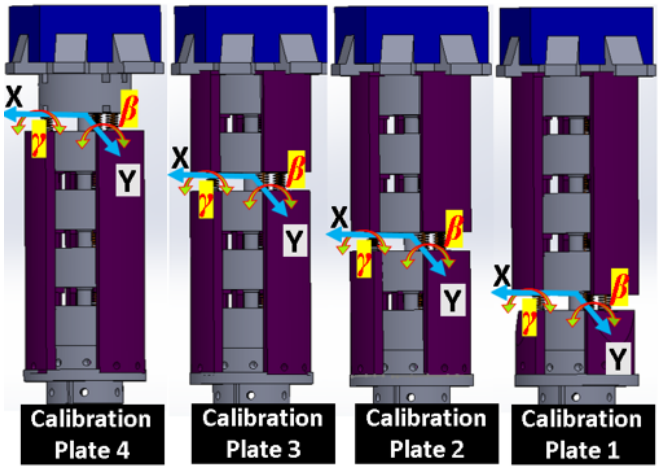

Fig.5. Multi-plate calibration method, by fixing sets of plates to allow only one to bend when actuated to collect all sensor data

For validation in a 4-unit section of the manipulator, each plate was calibrated separately. This was done using the set-up described in Fig.5. For the calibration of a plate, all other plates were fixed using interlocking components that prevent compression or extension of a unit when the tendons would be pulled. In the same manner to the single plate calibration process, a motion pattern would be generated by the control software to set the unit to move over the full angular range of ± 15 ° in both pitch and roll orientations, while sensor values are recorded. Again, an IMU was mounted above the top plate, to record all orientation values through the motion as the ground truth data. This is repeated for each plate. The data for each plate was passed through linear and non-linear regression models to calculate the coefficients as in (1)-(2). For validation of the calibration results, the full robotic manipulator is set to oscillate between a range of angles, up to maximum range of 60° in both pitch and roll orientations. Coefficients belonging to each set of plates are used to estimate pitch and roll of that plate, and these angles are consecutively summed to give the final orientation of the end plate. Results are shown in Figure 6, where the estimated orientations are compared against the real orientation data collected from the IMU sensor.

III. Analysis

With the presented single and four plate calibration validation experiments, the sensing principle using optoelectronic sensors can successfully be utilized for estimating orientation in a flexible robotic structure for shape sensing. In reference to Table I, and Fig 6, it is seen that a nonlinear regression model used to estimate orientation was more accurate than the linear regression model, with maximum percentage errors reducing

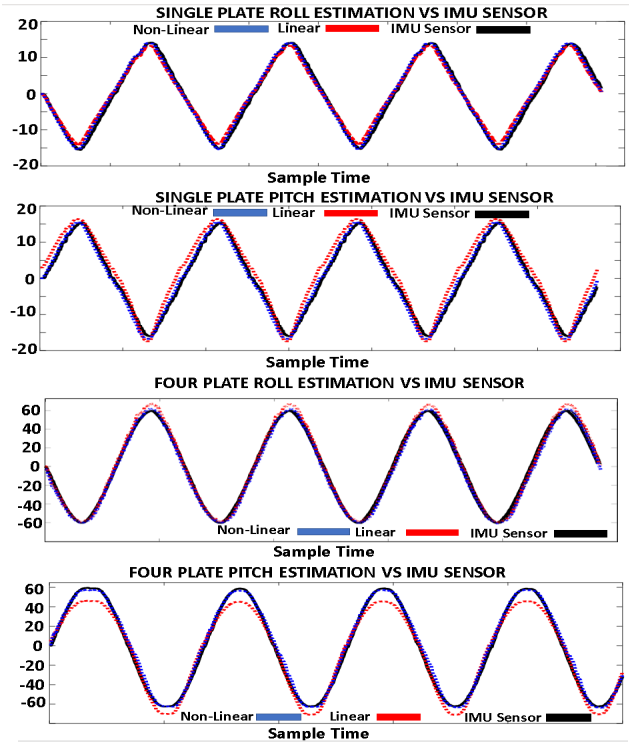

Figure 6. Results of single and four plate configurations with comparison of pitch and roll motions using two regression models against IMU data

from 4.57% to 0.69%. A similar trend is seen considering four plates, where orientations were tested to the maximum angular range of ±60°. Here the maximum percentage error seen for linear regression was 8.73% compared to only 1.31% for nonlinear regression estimations. As previously mentioned, the non-linear nature of the sensor with distance is cause for this trend. Although, when comparing to [1], we can see much improved accuracy with regards to the linear regression model, where maximum percentage errors fell from a reported 39.4% to 4.57% shown here for a single plate configuration, and from 33.8% to 8.73%, from a three plate to a four-plate configuration. This indicates that despite this weak regression model, the refined automated calibration platform allowed for significant increase in accuracy for shape sensing. An observation from the results is the increase in error when transforming from the single to four-plate configuration of the manipulator with both regression models. There may be many reasons for this. For example, the 3D printed PLA material used to construct the structure may have suffered some deformation during larger tensions required for the actuation of the four-plate configuration. This may have caused some unpredicted motion, leading to some unforeseen errors. PLA 3D printing resolution error may have also caused some small clearance between the joints of the plates which could have affected the motion. In future prototypes, alternative materials with more rigidity such as aluminium or stainless steel may be used to withstand excess tension and allow for a more precise fit. While fitted springs, alongside programmed motion control was used to limit yaw motion, another potential cause for errors may have been summations of small twist motions in each consecutive plate, causing an overall larger tip error. At this stage, only two orientations were considered – pitch and roll, however the

This article has been accepted for publication in a future issue of this journal, but has not been fully edited. Content may change prior to final publication. Citation information: DOI10.1109/TMRB.2022.XXXXXXX, IEEE Transactions on Medical Robotics and Bionics

intention is to eventually incorporate measurement to the third by geometrical design of the reflective surface for light modulation in this direction, with aim to boost the resulting shape sensing estimation accuracy. As this sensing technique is based on the modulation of light intensity, a soft material cover for the robotic manipulator to block external light signals will be included to exclude any ambient level light for better consistency.

TABLE I. SINGLE PLATE CALIBRATION RESULTS

Regression method	Orientation (±15°)	RMSE (°)	% Error
Linear	Pitch	2.45	4.57
	Roll	1.14	2.92
Non-Linear	Pitch	0.85	0.69
	Roll	0.76	0.46

TABLE II. FOUR PLATE CALIBRATION RESULTS

Regression method	Orientation (±60°)	RMSE (°)	% Error
Linear	Pitch	7.12	8.73
	Roll	3.44	4.41
Non-Linear	Pitch	3.23	1.31
	Roll	2.52	1.11

IV. Future Work

Following on from the work shown in this paper, the aim is to address the causes for error during calibration and motion control. Ultimately, the overall shape sensing system will be integrated onto a miniaturised robotic structure, for targeted applications in MIS. As mentioned in the design requirements, commercial trocar ports for multi-backbone continuum robots for surgery are found in the range of 10-15mm. With the shape sensing validated to maximum RMSE of 3.23° with non-linear fitting, this shows promising potential for applications in MIS with modification to target further accuracy. Smaller sensors will be employed such as the NJL5901R-2 (1 x 1.4 x 0.6 mm, New Japan Radio), as well as the use of ADCs (e.g., ADS1015, 1.5 x 2 x 0.4 mm, X2QNFT TEXAS IMSTRUMENT USA) which enable 4 electrical wires serially connected to transmit data and provide power to all the plates, thereby reducing the number of wires needed for the sensors. As such, a 10-15mm wide flexible robotic manipulator can feasibly be targeted, with increased plate numbers to extend workspace with reduced disk size. Such an approach may target more linear regions of the sensor variation curves with reduced rotation per plate, hence potential increase in estimation accuracy. With the sensing rooted in proximity-based intensity modulation, efforts can be made to adapt this shape sensing to other continuum robots such as single backbone, extensible or even concentric tube robots, by altering design through proximal variation to surfaces along the structure. In conclusion it can be said that there is great potential for further development of this shape sensor for MIS tools.

V. References

[1] J. H. Benjamin Koh, T. Jeong, S. Han, W. Li, K. Rhode, and Y. Noh, "Optoelectronic Sensor-based Shape Sensing Approach for Flexible Manipulators," *Proceedings of the Annual International Conference of the IEEE Engineering in Medicine and Biology Society, EMBS*, pp. 3199–3203, 2019.

[2] C. Shi, X. Luo, P. Qi, T. Li, S. Song, Z. Najdovski, T. Fukuda, and H. Ren, "Shape sensing techniques for continuum robots in minimally invasive surgery: A survey," *IEEE Transactions on Biomedical Engineering*, vol. 64, no. 8, pp. 1665–1678, 2017.

[3] Z. Zhang, J. Shang, C. Seneci, and G. Z. Yang, "Snake robot shape sensing using micro-inertial sensors," *IEEE International Conference on Intelligent Robots and Systems*, pp. 831–836, 2013.

[4] A. M. Franz, T. Haidegger, W. Birkfellner, K. Cleary, T. M. Peters, and L. Maier-Hein, "Electromagnetic tracking in medicine -A review of technology, validation, and applications," *IEEE Transactions on Medical Imaging*, vol. 33, no. 8, pp. 1702–1725, 2014.

[5] A. Schmitz, A. J. Thompson, P. Berthet-Rayne, C. A. Seneci, P. Wisanuvej, and G. Z. Yang, "Shape sensing of miniature snake-like robots using optical fibers," *IEEE International Conference on Intelligent Robots and Systems*, vol. 2017-Septe, pp. 947–952, 2017.

[6] F. al Jaber and K. Althoefer, "Towards creating a flexible shape senor for soft robots," *2018 IEEE International Conference on Soft Robotics, RoboSoft 2018*, no. 1, pp. 114–119, 2018.

[7] S. Sareh, Y. Noh, M. Li, T. Ranzani, H. Liu, and K. Althoefer, "Macrobend optical sensing for pose measurement in soft robot arms," *Smart Materials and Structures*, 2015.

[8] I. Floris, J. M. Adam, P. A. Calderón, and S. Sales, "Fiber Optic Shape Sensors: A comprehensive review," *Optics and Lasers in Engineering*, vol. 139, no. April, 2021.

[9] M. Amanzadeh, S. M. Aminossadati, M. S. Kizil, and A. D. Rakić, "Recent developments in fibre optic shape sensing," *Measurement: Journal of the International Measurement Confederation*, vol. 128, no. April, pp. 119–137, 2018.

[10] C. Shi, S. Giannarou, S. L. Lee, and G. Z. Yang, "Simultaneous catheter and environment modeling for Trans-catheter Aortic Valve Implantation," *IEEE International Conference on Intelligent Robots and Systems*, no. Iros, pp. 2024–2029, 2014.

[11] R. J. Roesthuis, S. Janssen, and S. Misra, "On using an array of fiber Bragg grating sensors for closed-loop control of flexible minimally invasive surgical instruments," *IEEE International Conference on Intelligent Robots and Systems*, pp. 2545–2551, 2013.

[12] S. C. Ryu and P. E. Dupont, "FBG-based shape sensing tubes for continuum robots," *Proceedings - IEEE International Conference on Robotics and Automation*, pp. 3531–3537, 2014.

[13] R. Li, Y. Tan, Y. Chen, L. Hong, and Z. Zhou, "Investigation of sensitivity enhancing and temperature compensation for fiber Bragg grating (FBG)-based strain sensor," *Optical Fiber Technology*, vol. 48, no. November 2018, pp. 199–206, 2019.

[14] S. Sareh, Y. Noh, T. Ranzani, H. Wurdemann, H. Liu, and K. Althoefer, "A 7.5mm Steiner chain fibre-optic system for multi-segment flex sensing," *IEEE International Conference on Intelligent Robots and Systems*, vol. 2015-Decem, pp. 2336–2341, 2015.

[15] J. R. Romanelli and D. B. Earle, "Single-port laparoscopic surgery: An overview," *Surgical Endoscopy*, vol. 23, no. 7, pp. 1419–1427, 2009.

[16] J. Burgner-Kahrs, D. C. Rucker, and H. Choset, "Continuum Robots for Medical Applications: A Survey," *IEEE Transactions on Robotics*, vol. 31, no. 6, pp. 1261–1280, 2015.

[17] F. Li, "DESIGN AND ANALYSIS OF A FINGERTIP STEWART PLATFORM FORCEITORQUE SENSOR," no. March, 1998.